FASTC-ID(RS)T-0785-91

(2)

FOREIGN TECHNOLOGY DIVISION

CARBON/CARBON COMPOSITION ABLATION EFFECTS ON IONIZED BOUNDARY LAYERS

by

Wei Shuru, Wang Ce, Wang Fuhan

Approved for public release;
Distribution unlimited.

HUMAN TRANSLATION

FTD-ID(RS)T-0785-91 13 January 1992

CARBON/CARBON COMPOSITION ABLATION EFFECTS ON IONIZED BOUNDARY LAYERS

By: Wei Shuru, Wang Ce, Wang Fuhan

English pages: 6

Source: Kongqidonglixue Xuebao, Vol. 7, Nr. 4. 1989, pp. 413-416

Country of origin: China
Translated by: SCITRAN
F33657-87-D-0165
Requester: FASTC/TTTAV/Capt Phillips

GRAPHICS DISCLAIMER

All figures, graphics, tables, equations, etc. merged into this translation were extracted from the best quality copy available.

TITLE: CARBON/CARBON COMPOSITION ABLATION EFFECTS ON IONIZED BOUNDARY LAYERS

AUTHOR: Wei Shuru Wang Ce Wang Fuhan

Abstract A calculation method for carbon/carbon composition thermochemical ablation effects on ionized laminar and turbulent boundary layers is given. In the boundary layers 20 gas species are considered and all chemical reactions which occured in them are assumed to be equilibrium. The new solving method for boundary layer equations and simple disposal for transport properties are applied. The calculation examples indicate that ablation has great effects on ionization properties of the boundary layers and that ionizations of the alkaline metals are not always dominant.

Key words ablation, ionization, boundary layer, laminar, turbulent.

V. SAMPLE CALCULATIONS AND ANALYSIS

We used Reference [11]'s sample calculations and sample calculations for other object forms as well as flight conditions to carry out calculations. A part of the results are as shown in Fig.1-3. From the results of calculations, it is possible to obtain:

(1) Combustion corrosion or ablation has a very great influence on boundary layer ionization characteristics. At analogous or corresponding points (for example, wall surfaces), the ablation values for electron number densities are highest as compared to pure air values under the same conditions by 3-4 orders of magnitude[9] (See Fig.1). The peak values in boundary layers are 1-2 orders of magnitude higher (Fig.2). 414

(2) The introduction of ablation products causes electron number density cross sections to tend toward saturation, that is to say, the high density regions get thicker, turbulent flow boundary layers in particular (Fig.2).

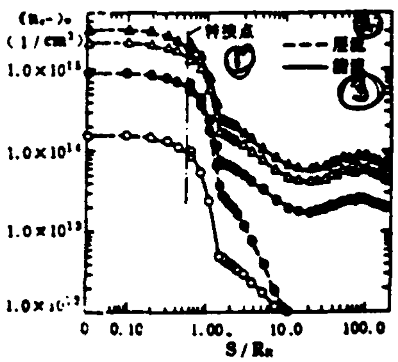

图1 烧蚀壁面电子数密度分布

● $\tilde{K}_{Nac}$ = 100 ppm △ $\tilde{K}_{Nac}$ = 500ppm

▲ $\tilde{K}_{Nac}$ = 1000 ppm ○ 纯空气

Fig.1 Ablation Wall Surface Electron Number Density Distribution (1) Turning or Transition Point (2) Laminar Flow (3) Turbulent Flow (4) Pure Air

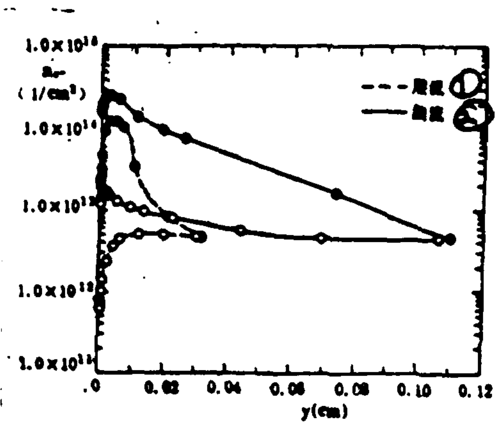

图 2　边界层中电子数密度分布

● $\tilde{K}_{Nac} = 100$ ppm　　○ 纯空气 3

$S/R_N = 2.35$　　$P_e = 7.7499 \times 10^6$ Pa

$u_e = 2.8678 \times 10^3$ m/s　　$h_e = 4.9610 \times 10^6$ J/kg

$R_N = 1.27$ cm

Fig.2 Distribution of Electron Number Density in Boundary Layers (1) Laminar Flow (2) Turbulent Flow (3) Pure Air

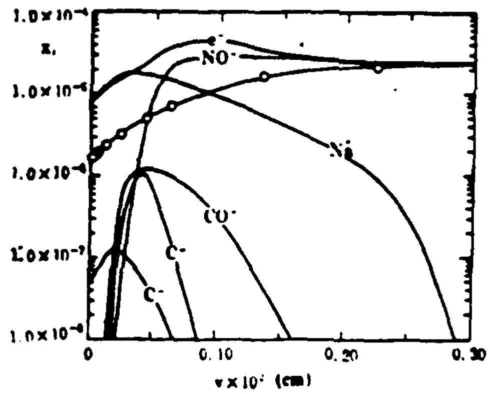

图 3(a)

1

○ 空气边界层的x_e 2　　$\tilde{K}_{Nac} = 100$ ppm

$S/R_N = 0.00$(驻点层流)　　$R_N = 1.27$ cm

$P_e = 1.5190 \times 10^7$ Pa　　$T_w = 4417.2$ K

$u_e = 0.00$ m/s　　$\dot{m}_w = 0.2789$ g/cm²-s

$h_e = 9.0730 \times 10^6$ J/kg

3(a) (1) Air Boundary Layer (2) Stationary Point Laminar Flow

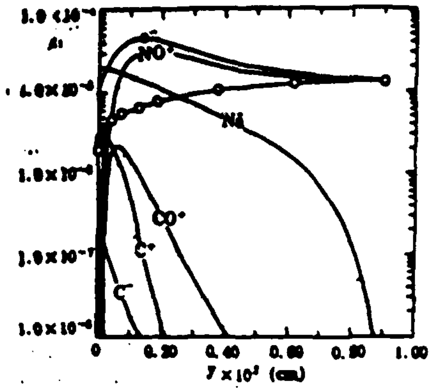

图 3(b)

(1)

○ 空气边界层的x_e | $\tilde{K}_{Nae}$ = 100 ppm
S/R_N = 0.60(湍流)(2) | R_N = 1.27 cm
P_e = 9.7110×10^{6} Pa | T_W = 4427.0 K
u_e = 1.2343×10^{3} m/s | $\dot{m}_w$ = 0.8955 g/cm²·s
h_e = 7.8830×10^{6} J/kg

Fig.3(b) (1) Air Boundary Layer (2) Turbulent Flow

415

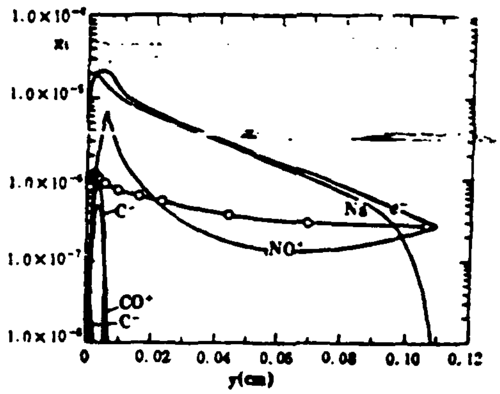

图 3(c)

(1)

○ 空气边界层的x_e | $\tilde{K}_{Nae}$ = 100 ppm
S/R_N = 2.35 湍流 (2) | R_N = 1.27 cm
P_e = 7.7499×10^{5} Pa | T_W = 3831.9 K
u_e = 2.8678×10^{3} m/s | $\dot{m}_w$ = 0.1465 g/cm²-s
h_e = 4.9610×10^{6} J/kg

Fig.3(c) (1) Air Boundary Layer (2) Turbulent Flow

(3) Within ablation wall surfaces and their adjacent thin layers, electrons, generally speaking, come mainly from ablation products, in particular, ions from alkali metals. However, in most of the depth of boundary layers, as far as whether air components or ablation products occupy the dominant postion in ionization mechanisms

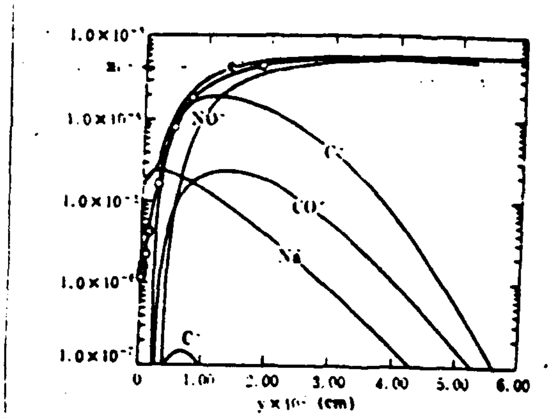

图 3(d)

① ○ 空气边界层的 x_e

② $S/R_N = 0.00$(驻点层流)

$P_e = 5.60 \times 10^{[illegible]}$ Pa

$u_e = 0.00$ m/s

$h_e = 22.44 \times 10^{[illegible]}$ J/kg

$\bar{K}_{Nac} = 100$ ppm

$R_N = 6.00$ cm

$T_W = 3888.7$ K

$\dot{m}_w = 0.03329$ g/cm²·s

Fig.3(d) (1) Air Boundary Layer (2) Sationary Point Laminar Flow

Fig.3 Mol Fraction Cross Sections for Charged Components

is concerned, it is still decided by the conditions of flight and the locations at which the boundary layers find themselves. Generally speaking, stationary point laminar flows, even to include turning or transition points, hold relatively close to past turbulent flows, and air components are dominant (Fig.3(a), (b), and (d)). However, in the lower reaches of the flow, by contrast, ablation products hold the dominant postion (Fig.3(c)). As far as the ionization component which occupies the dominant position is concerned, the rules or patterns for the transition from air to ablation products are somewhat similar to the rules or patterns for boundary layer transitions. However, the points of change are all in the reaches of the flow below the boundary layer transition points.

(4) Among ablation products, alkali metal ionization most certainly does not occupy the dominant postion overall. Among the boundary layers of spherical tip regions when flying at relatively high altitudes, the relevent contributions of CO^+--in particular C^+--(this refers to X_{C+}/X_{e-}, and so on), at times, reach even as high as 70% (Fig.3(d)). These mechanisms have important effects on

raising electron number density peak values and increasing the thicknesses of high concentration regions.

REFERENCES

[1] Blottner, F.G., *AIAA J.* 8, 2(1970), 193—205.

[2] Huheaode (phonetic), et.al.: "Tip Cover Plasma Analysis of Spheroconical Long Thin Objects", Acta Aerodynamica Sinica, 1, 4(1983), 77-85

[3] Wei Shuru, Wang Fuhan, and Wang Ce; "Ionized Air Equilibrium Boundary Layers", Acta Aerodynamica Sinica, 7, 2(1989), "183-191

[4] Bartlett, E.P. & Kendall, R.M., NASA CR-1062 (1968).

[5] Duo Lansi; "Hypersonic Viscous Flows", National Defense Industry Press, (1966), 193-203

[6] Tong, H., et al, NASA N73-31835 (1973).

[7] Wei Shuru, et.al.; "One Type of New Solution Method for Boundary Layer Equations", Mechanics Journal, 19, extra, (1987), 55-63

[8] Putz, K.E. & Bartlett, E.P., AIAA Paper 72—91.

[9] Wei Shuru, et.al.; "Ablation of Carbonized Materials in Ionized Air Environments", Acta Aerodynamica Sinica, 4, 4(1986), 352-360

[10] Глушко, В.П., И др., Термодинамические свойства индивидуальных веществ, ТОМ I-ТОМ IV, «НАУКА», МОСКВА (1979—1982).

[11] Anderson, L.W. & Morse, H.L., AD-734744, (1971).

DISTRIBUTION LIST

DISTRIBUTION DIRECT TO RECIPIENT

ORGANIZATION	MICROFICHE
B085 DIA/RTS-2FI	1
C509 BALLOC509 BALLISTIC RES LAB	1
C510 R&T LABS/AVEADCOM	1
C513 ARRADCOM	1
C535 AVRADCOM/TSARCOM	1
C539 TRASANA	1
Q592 FSTC	4
Q619 MSIC REDSTONE	1
Q008 NTIC	1
Q043 AFMIC-IS	1
E051 HQ USAF/INET	1
E404 AEDC/DOF	1
E408 AFWL	1
E410 ASDTC/IN	1
E411 ASD/FTD/TTIA	1
E429 SD/IND	1
P005 DOE/ISA/DDI	1
P050 CIA/OCR/ADD/SD	2
1051 AFIT/LDE	1
CCV	1
P090 NSA/CDB	1
2206 FSL	1

Microfiche Nbr: FTD92C000051
FTD-ID(RS)T-0785-91